Am J Transl Res 2016;8(2):460-472
www.ajtr.org /ISSN:1943-8141/AJTR0018266

Original Article

Protective role of propofol on the kidney during early unilateral ureteral obstruction through inhibition of epithelial-mesenchymal transition

Li Song[1*], Sen Shi[2*], Wei Jiang[3], Xueru Liu[1], Yanzheng He[2]

[1]Department of Anesthesiology, Affiliated Hospital of Southwest Medical University, Luzhou, Sichuan 646000, China; [2]Department of Vascular and Thyroid Surgery, Affiliated Hospital of Southwest Medical University, Luzhou, Sichuan 646000, China; [3]Department of Rehabilitation, Affiliated Hospital of Southwest Medical University, Luzhou, Sichuan 646000, China. [*]Equal contributors.

Received October 21, 2015; Accepted January 6, 2016; Epub February 15, 2016; Published February 29, 2016

Abstract: Unilateral ureteral obstruction (UUO) induces functional and pathological changes in the obstructed kidney. Inducible nitric oxide synthase (iNOS) expression is high inearly UUO mouse kidney, which is accompanied with fibrosis. Propofol has preventive effects against renal injury by downregulating iNOS expression in UUO mouse models. However, the role of propofol in kidney fibrosis progression has not been reported. We explored the therapeutic potential and possible mechanisms of action of propofol in kidney fibrosis using a UUO mouse model. Herein, mice anesthetized with propofol or sevoflurane underwent UUO induction. Serum and kidney sections were collected 5 and 28 days post-operation for histological, morphometric, immunofluorescence, microRNA analyses; quantitative PCR and western blotting. In vivo, the effect and mechanism of propofol on epithelial-mesenchymal transition (EMT), transforming growth factor β (TGF-β) signaling and miR-155 levels were detected in cultured HK-2 cells. We found that propofol significantly suppressed UUO-induced kidney fibrosis, which was associated with TGF-β/Smad3 signaling, EMT, and iNOS-NO production. MiR-155 levels were higher in UUO mouse kidneys; compared with sevoflurane, propofol suppressed miR-155 levels. However, in late UUO, propofol could not prevent kidney fibrosis or suppress EMT and miR-155. The *in vitro* results showed that propofol suppressed TGF-β1-induced EMT by regulating miR-155 levels. As a conclusion, in early UUO mice, propofol may inhibit TGF-β1 expression and NO-iNOS production, consequently inhibiting EMT and kidney fibrosis by regulating miR-155 levels, and might be a new protective agent against kidney injury during surgery and in therapy to prevent kidney fibrosis.

Keywords: Epithelial-mesenchymal transition (EMT), inducible nitric oxide synthase (iNOS), miR-155, propofol, unilateral ureteral obstruction (UUO)

Introduction

Kidney fibrosis, characterized by excessive extracellular matrix (ECM) deposition, is a common pathological feature of chronic kidney diseases (CKD) thatleads to the development of end-stage renal disease (ESRD), accompanied by a progression of renal malfunctions [1, 2]. Although effective therapy for renal fibrosis is lacking, transforming growth factor β (TGF-β) is the key mediator in kidney disease associated with progressive renal fibrosis [3]. The significance of TGF-β-induced epithelial-mesenchymal transition (EMT) in organ fibrosis progression has been demonstrated using bone morphogenetic protein-7, a TGF-β signaling antagonist, in mouse models of kidney, liver, biliary tract, lung, and intestinal fibrosis [4]. Inflammatory injury to mouse kidney results in the recruitment of diverse cells that can trigger EMT through their release of growth factors such as TGF-β, platelet-derived growth factor, epidermal growth factor (EGF), and fibroblast growth factor-2 [5]. Tubular EMT could be purposefully orientedinto a constructive pathway torepair kidney injury via tubular regeneration, matrix remodeling, andtissue structure and function restoration. Importantly, EMT occursnot only in CKD, but also in acute kidney injury (AKI) [6].

MicroRNAs (miRNAs), a novel class of post-transcriptional regulators of gene expression, are usually inhibitory and might be involved in regulating the acute inflammatory processes [7]. TGF-β induces miR-155 expression and promoter activity through Smad4. MiR-155 knockdown suppresses TGF-β-induced EMT and tight junction dissolution, cell migration and invasion [8]. Compared with controls, miR-155 expression was increased by >5-fold in the kidney samples of patients with diabetic nephropathy, and miR-155 expression is closely correlated with serum creatinine levels, which subsequently increase tumor necrosis factor-α (TNFα), TGF-β1, and nuclear factor-κB (NF-κB) expression [9].

A highly lipid-soluble anesthetic, propofol (2,6-diisopropylphenol) has potent antioxidant activity against lipid peroxidation both *in vitro* and *in vivo* [10, 11]. In a unilateral ureteral obstruction (UUO) mouse model, propofolprevents renal injury by down-regulating inducible nitric oxide synthase (iNOS) expression [11]. The TGF-β1/phosphatidylinositol 3-kinase (PI3K)/Akt pathway mediates increased iNOS, at least partially [12]. Moreover, propofol protects HK-2 human kidney proximal tubular epithelial cells against H_2O_2-induced oxidative stress *in vitro*. TGF-β1 is a key factor in kidney fibrosis, and iNOS expression is high inearly UUO mouse kidneys, whichis accompanied with fibrosis [13]. However, the role of propofol in kidney fibrosis progression has not been reported. Herein, we explored the therapeutic potential and possible mechanisms of propofol in kidney fibrosisina UUO model, examining the effects of propofol on TGF-β-mediated EMT in HK-2 cells and in a mouse model of UUO renal fibrosis.

Methods

Animals

The Southwest medical university Animal Investigation Committee approved the experimental protocol, which adhered to National Institutes of Health guidelines for the use of experimental animals. Male BALB/c mice (20-25 g) were purchased from the Sichuan University Experimental Animal Center and housed in individual cages in acohorted temperature-controlled room with alternating 12-h light/dark cycles, and acclimated for a week before the study. The mice were randomly divided into four groups: (1) sham operationwith propofolanesthesia; (2) UUO with propofolanesthesia; (3) sham operation with sevofluraneanesthesia; (4) UUO with sevoflurane anesthesia (*n* = 6 per group).

Anesthesia

Mice in the sevoflurane groups were placed in an acrylic glass chamber (FiO_2 = 0.4; T = 32°C) pre-flushed with 5.0 vol% sevoflurane to induce anesthesia. After loss of postural reflexes, the anesthetized animal was removed from the chamber. Propofol (50 mg/kg) was administered via the tail vein [14], and mice were placed in the same anesthetic chambers as above with humidified 30% oxygen at 38°C. The anesthesia maintenance time was defined as the time between loss and recovery of the righting reflex, i.e., the ability to perform three successive righting reflexes. The duration of anesthesia was approximately 150 min from induction until procedure ended.

UUO model

After induction of anesthesia, the mice were placed on a heated table to maintain arectal temperature of 37-38°C. The depthof surgical anesthesia was assessed by checking the interdigital (pedal) reflex using surgical forceps. This reflex was absent from both the fore- and hind legs. In UUO induction, the abdominal cavity was exposed by a midline incision, and the left ureter was isolated and ligated with 5-0 silk at two points. Controls (sham operation groups) underwent an identical surgical procedure without ureteral ligation. At 5 and 28 days post operatively, the animals were sacrificed by propofolorsevoflurane overdose based on their initial grouping, and the kidneys were removed for biochemical analysis and pathological evaluation.

Immunofluorescence

Frozen kidney sections (5-μm thickness) were used for immunofluorescence studiesto measure the double-positive labeling of E-cadherin and α-SM actin (αSMA). Briefly, frozen sections were dried and placed in acetone for 10 min at -30°C, blocked with 2% BSA/PBS for 30 min at room temperature, incubated in primary antibody for 1 h, and washed 5 min, thrice, in phos-

phate-buffered saline (PBS). Next, the sections were incubated with secondary antibodies for 30 min, washed with PBS thrice, and mounted with mounting medium containing diaminophenylindole (DAPI; Vector Laboratories, Burlingame, CA). The immunolabeled sections were analyzed using fluorescence microscopy (Axio Vert. A1; Carl Zeiss Microscopy GmbH, Jena, Germany). We obtained ×300 magnification images from six different fields per mouse.

Morphological evaluation

Morphological evaluation was performed as previously described [15]. Briefly, the glomerular surface area was calculated with 10 glomeruli per mouse using ImageJ. To evaluate the mesangial matrix area (%), we utilized a point counting method, where 10 periodic acid–Schiff (PAS)-stained glomeruli per mouse were analyzed on a digital microscope screen grid containing 540 (27 × 20) points in Adobe Photoshop Element 7. The number of grid points in the mesangial area was divided by the total number of points in the glomerulus to obtain the relative mesangial matrix area (%) in a given glomerulus. Masson's trichrome (MTS)-labeled sections were imaged and analyzed with ImageJ; fibrotic areas were quantified. We evaluated six images (× 300 magnification) per mouse.

Cell culture

Immortalized HK-2 cells (American Type Culture Collection, Manassas, VA) were grown and passaged in 25-cm^2 cell culture flasks containing culture medium (keratinocyte serum–free medium, 5 ng/mL EGF, 40 mg/mL bovine pituitary extract; Gibco BRL, Grand Island, NY) and antibiotics (100 U/mL penicillin G, 100 μg/mL streptomycin, 0.25 μg/mL amphotericin B). Cultured cells were incubated at 37°C in a 100% humidified incubator containing 5% CO_2. Cells were plated in 6-well plates at 80% confluence, and culture medium was replaced every twodays. Cells that were 70% confluent were pre-incubated with 50 μM propofol for 30 min, and then treated with TGF-β1 (10 ng/mL; R&D Systems, Minneapolis, MN). Propofol was dissolved in dimethyl sulfoxide (Sigma-Aldrich, St. Louis, MO, to a final concentration in medium of 0.0025-0.0125% [16]. After 48 h, cells were harvested for western blotting and quantitative PCR (qPCR) analysis.

Real-time reverse transcription-PCR (RT-PCR) and miRNA analysis

Total RNA was extracted from kidney tissue using TRIzol (Invitrogen, Carlsbad, CA) according to the manufacturer's instructions. RT-PCR was performed in 25-μL reactions containing 10 pmol primers, and E-cadherin and αSMA expression levels were detected using an ABI Prism 7300 Sequence Detection System (Applied Biosystems, New York, NY). The following PCR primers were used: E-cadherin forward, 5'-ACAGCCCCGCCTTATGATT-3'; E-cadherin reverse, 5'-TCGGAACCGCTTCCTTCA-3'; αSMA forward, 5'-GTCCACCGCAAATGCTTCTAA-3'; αSMA reverse, 5'-AAAACACATTAACGAGTCAG-3'; TGF-β1 forward, 5'-GCTTCAGACAGAAACTCACT-3'; TGF-β1 reverse 5'-GAACACTACTACATGCCATT-AT-3'; miR-155 forward, 5'-CTCGTGGTTAATGC-TAATTGTGA-3'; and miR-155 reverse, 5'-GTGCAGGGTCCGAGGT-3'. The experiments were performed in triplicate. Relative mRNA expression levels were calculated using 18S as thereference gene. Each miRNA expression was normalized using U6 as the internal control; group differences were calculated as the inverselog of the comparative threshold cycle (ΔΔCt) to yield the relative foldchange in miRNA levels. Each miRNA PCR was repeated thrice using separate reaction mixtures.

Western blot analysis

Kidney sections were prepared in a lysis buffer containing 0.5 M NaF, 0.1 M Na_3VO_4, and protease inhibitor cocktail. Protein lysates were separated on sodium dodecyl sulfate-polyacrylamide gel (SDS-PAGE) and blotted onto polyvinylidene difluoride (PVDF) membranes (Pall Corporation, Pensacola, FL) using semidry transfer. After blocking with 5% BSA/TBST, the membranes were incubated with 1:1000 primary antibodies (controls: β-actin and glyceraldehyde-3-phosphate dehydrogenase [GAPDH], 1:10000) at 4°C overnight. The membranes were washed thrice and incubated with 1:2000 horseradish peroxidase-conjugated secondary antibodies for 1 h at room temperature. Immunoreactive bands were visualized using an enhanced chemiluminescence (ECL) detection system (Pierce Biotechnology, Rockford, IL) and Image Quant LAS 400 (GE Healthcare Life Sciences, Uppsala, Sweden).

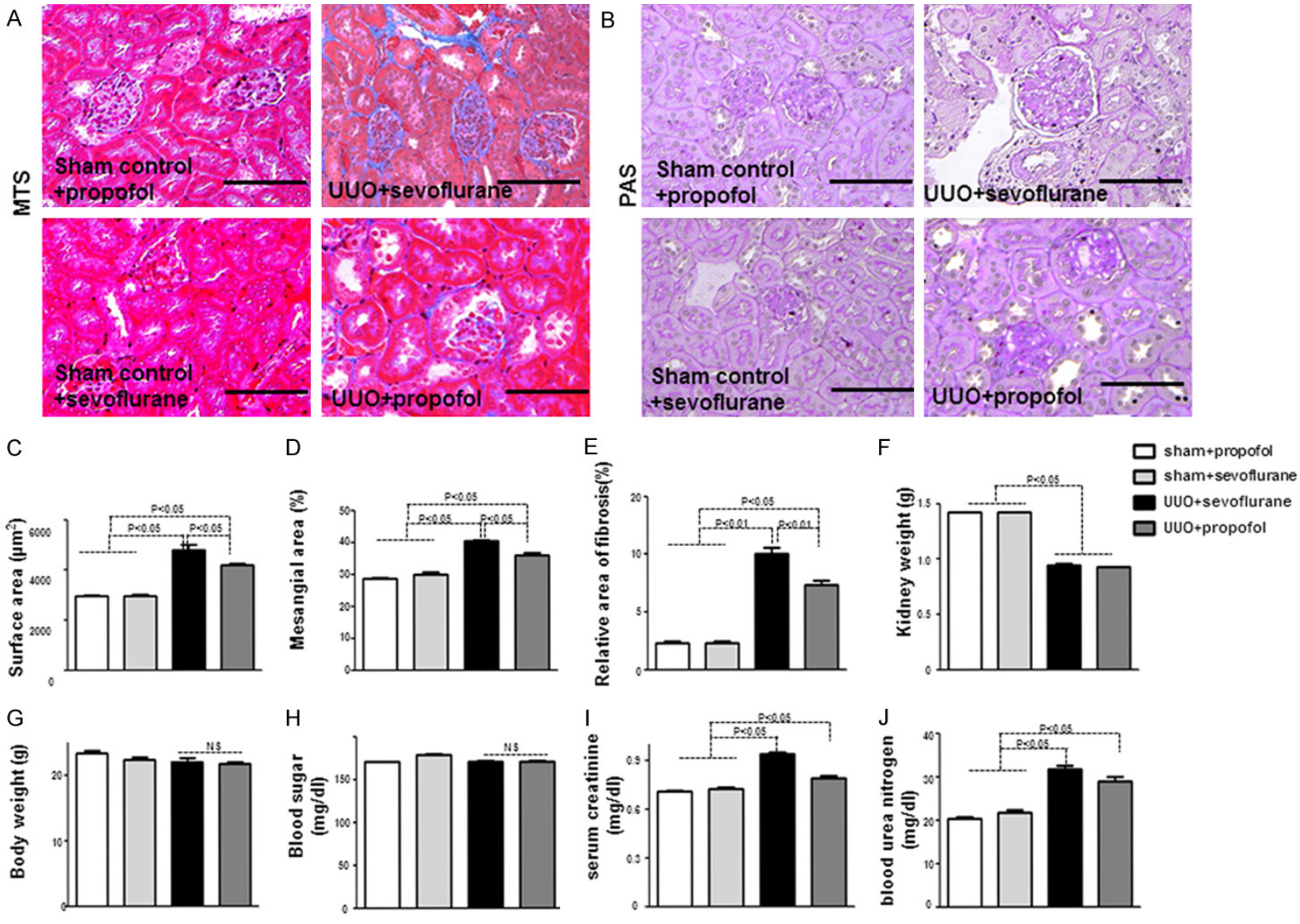

Figure 1. Propofol ameliorates early UUO-induced kidney fibrosis. A. MTS staining in mouse kidney. Scale bar: 50 μm. B. PAS staining of glomeruli. Scale bar: 50 μm. C-E. Morphometric analysis of kidney histology (n = 5 per group). F-J. Characteristics and kidney function in mice (n = 5). F. Kidney weight (right and left); G. Body weight; H. Blood sugar; I. Serum creatinine; J. BUN.

Quantification of TGF-β1

HK-2 cells were cultured in medium containing 5 mM glucose for 48 h before overnight serum starvation. Cells were stimulated for 24 h with 50 μM propofol under serum-free conditions; total TGF-β1 was measured by specific enzyme-linked immunosorbent assay (Abcam, Cambridge, UK) of cell culture supernatant collected from growth-arrested HK-2 cells. TGF-β1 concentrations were normalized to mg/mL protein. Data were obtained as pictograms of TGF-β1 per mL/mg protein and expressed as the percentage as compared to the control.

Determination of tissue NO levels

Kidney NO production was quantified indirectly as the nitrite/nitrateratio in kidney homogenates based on the Griess method, using 2-10 μM sodium nitrite or sodium nitrate as the standards [17]. The data reported represent the sum of nitrite and nitrate and are expressed as μmol NO per g wet tissue (μmol/g).

Statistical analysis

For western blot analysis, the raw data were adjusted with GAPDH or β-actin, for microRNA analysis, the raw data were adjusted with 18s. All the data were expressed as the means ± standard error of the mean (SEM). Statistical comparisons among the treatment groups were performed using randomized-design two-way analysis of variance followed by the Newman-Keuls post hoc test for more than two groups or unpaired Student's t test for two groups using Prism software (GraphPad Inc., La Jolla, CA, USA) as appropriate. Statistical significance was defined as $P < 0.05$.

Results

Propofol ameliorated early UUO-induced kidney fibrosis

UUO mice developed kidney fibrosis, with tubulointerstitial fibrosis occurring approximately five days post-operation (**Figure 1A-E**); 28 days post-operation, UUO mice had severe fibrosis as compared with control mice (Supplementary Figure 1A, 1B). Compared to sevoflurane+UUO mice at five days, propofol+UUO mice exhibited restored normal kidney structure (**Figure 1A**, **1B**). Morphometric analysis of UUO mouse kidneys revealed significantly enlarged glomeruli, mesangial expansion, and relative areas of MTS-positive interstitial fibrosis (**Figure 1C-E**); in UUO mice, when compared with sevoflurane group, propofol restored normal kidney histology and architecture at five days (**Figure 1C-E**); both propofol+UUO and sevoflurane+UUO mice had fibrotic kidney histology and architecture at 28 days (Supplementary Figure 1A, 1B). UUO mice had lower kidney weight compared to the controls (**Figure 1F**); compared with sevoflurane, propofoldid not alter UUO mice body weight, blood sugar levels, or kidney weight (**Figure 1F**, **1G**). Serum creatinine and blood urea nitrogen (BUN) were elevated in UUO mice; in UUO mice, when compared with sevoflurane group, propofol suppressed the trend for increased serum creatinine (**Figure 1I**, **1J**).

Thepropofol anti-fibrotic effect was associated with suppressed TGF-β/smad signaling in early UUO mouse kidney

TGF-β/Smad signaling plays an important role in renal fibrosis. Targeting TGF-β/Smad3 signaling may represent specific and effective therapy for renal fibrosis [18]. We analyzed TGF-β1 expression at five days in UUO mouse kidney; immunohistochemistry revealed that TGF-β1 was significantly higher in UUO mice than in control mice (**Figure 2A**); among the UUO mice, when compared to the sevoflurane group, TGF-β1 expression was obviously suppressed in the propofol group (**Figure 2A**). Western blotting and qPCR showed similar results for kidney TGF-β1 protein and mRNA levels (**Figure 2B**, **2D**, **2G**). Furthermore, phosphorylated Smad3 (p-Smad3) was increased in UUO mice when compared with the controls; compared with sevoflurane group, propofol decreased p-Smad3 in UUO mice (**Figure 2F**). In diabetic rats, NO levels are significantly increased in the early stages of kidney disease [19-21] and NO overproduction is related to TGF-β1/PI3K/Akt pathway activation [12]. We also analyzed iNOS protein and NO levels, andfound significantly increased NO in UUO mouse kidney at five days; compared with sevoflurane group, propofoldecreased the NO and iNOS levels in UUO mice (**Figure 2B**, **2E**, **2H**). However, NO and iNOS levels were decreased at 28 days in UUO mice as compared with the controls, while propofol+UUO and sevoflurane+UUO mice did

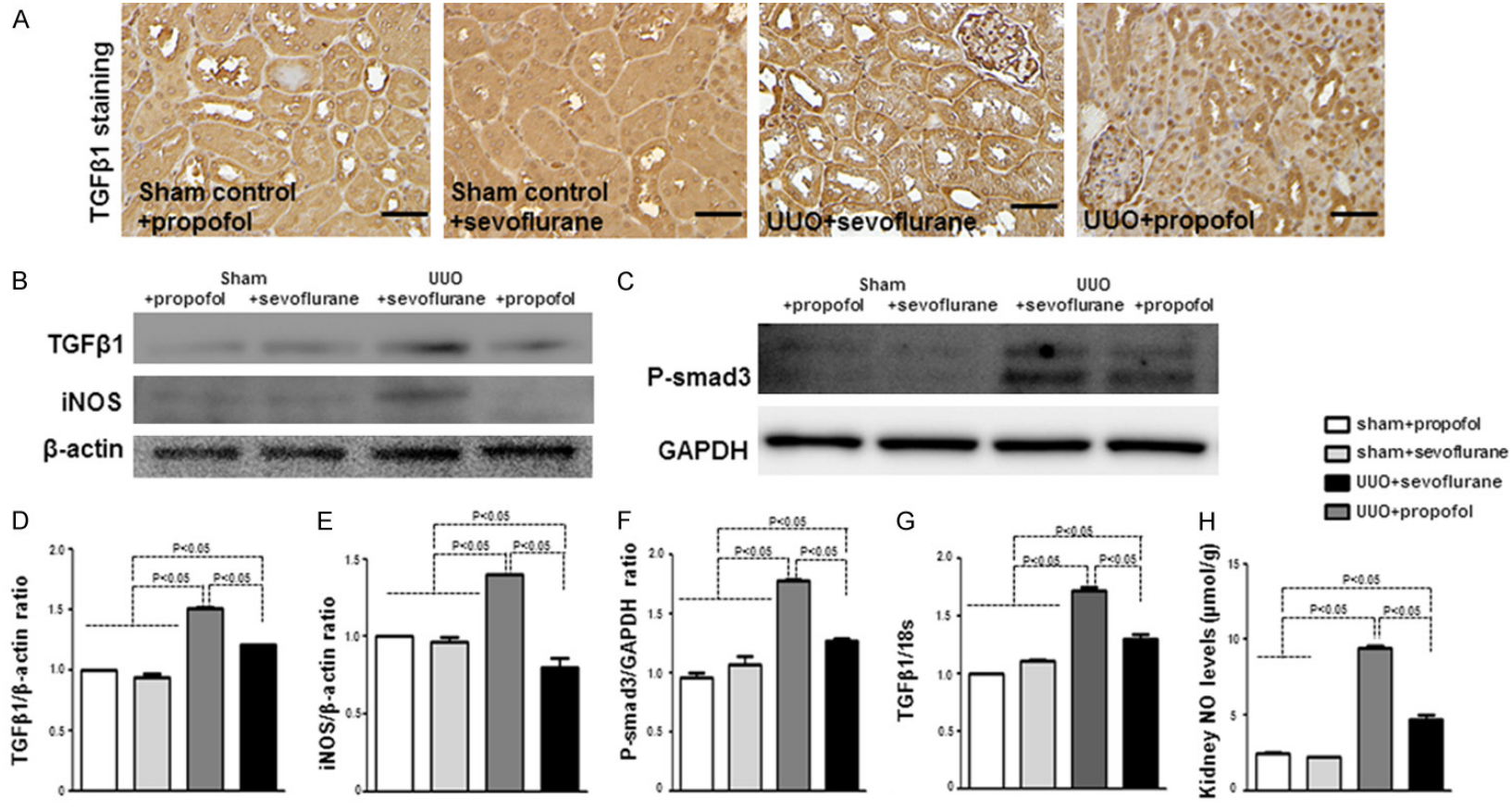

Figure 2. The anti-fibrotic effect of propofol is associated with suppression of TGF-β/Smad signaling in early UUO mousekidney. A. Immunohistochemical analysis of TGF-β1 (n = 5 per group). Scale bar: 50 μm. B, C. Western blot analysis of TGF-β1, iNOS, and p-Smad3. Representative blots from four independent experiments are shown. D-F. Densitometric analysis of protein expression relative to β-actin levels (n = 4 per group). G. qPCR analysis of TGF-β1 in the kidneys (n = 5 mice per group). H. Analysis of NO levels in the kidneys (n = 5 per group). Data are the means ± SEM.

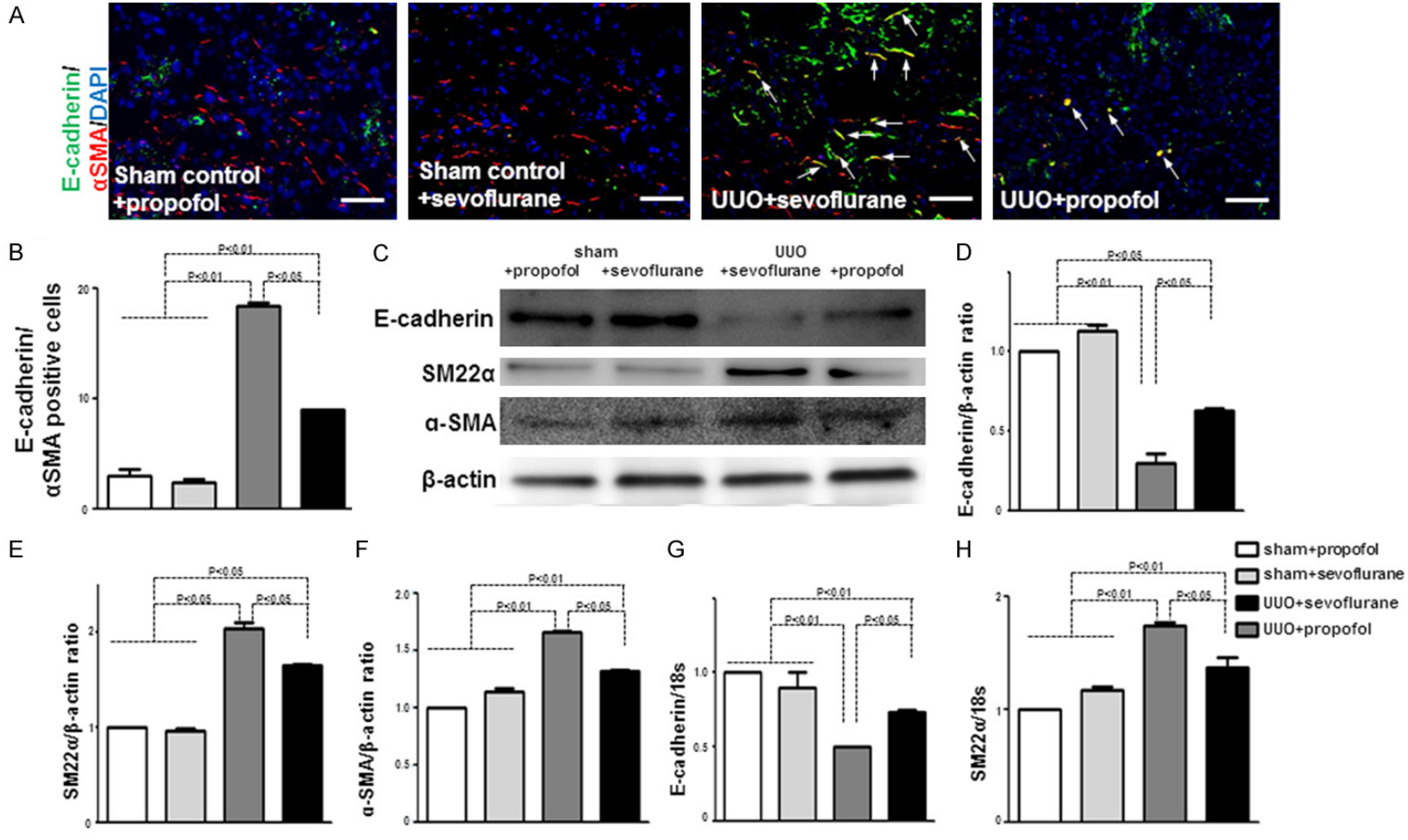

Figure 3. Propofol inhibits EMT in early UUO mouse kidney. A. E-cadherin and αSMA immunolabeling visualized by fluorescence microscopy. Arrows indicate cells undergoing EMT. Scale bar: 50 μm (n = 5 per group). B. Quantification of E-cadherin-αSMA double-positive cells. The percentages of cells undergoing EMT were calculated among all DAPI-positive cells (n = 5 per group). C. Western blot analysis of E-cadherin, SM-22α, and αSMA inkidney samples. Protein lysates (15 μg) wereseparated by PAGE and transferred onto PVDF membranes. Immunoreactive bands were analyzed by ECL. Representative data from fourmice per group are shown. D-F. Densitometric analysis of E-cadherin, SM-22α, and αSMA; western blot analysis normalized the levels with β-actin (n = 4 per group). Data are the means ± SEM. G. qPCR analysis of E-cadherin in the kidneys (n = 5 mice per group). H. qPCR analysis of SM-22α in the kidneys (n = 5 mice per group).

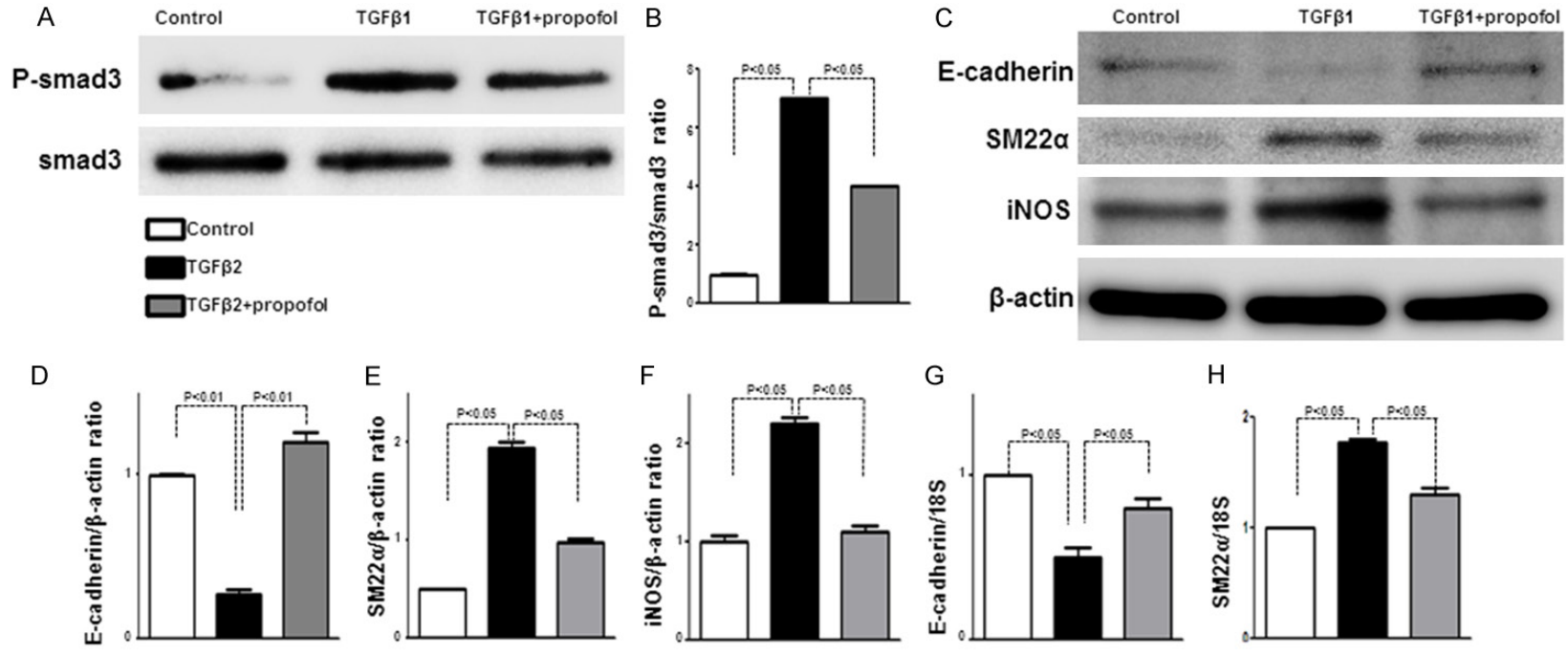

Figure 4. Propofol inhibits EMT and iNOS in HK-2 cells. A. Western blot analysis of p-Smad3 in HK-2 cells. Representative data from four bands per group are shown. B. Densitometric analysis of p-Smad3 normalized to Smad3 (n = 4 per group). Data are the means ± SEM. C. Western blot analysis of E-cadherin, SM-22α, and iNOS in HK-2 cells. D-F. Densitometric analysis of E-cadherin, SM-22α, and iNOS normalized to β-actin (n = 4 per group). Data are the means ± SEM. G. qPCR analysis of E-cadherin in HK-2 cells. H. qPCR analysis of SM-22α in HK-2 cells.

not differ significantly (Supplementary Figure 2A, 2B).

Propofol inhibited EMT in kidney of UUO mice

Kidney fibroblasts play essential roles in kidney fibrosis and originate from diverse sources [22, 23]. Here, we analyzed EMT, an important source of kidney fibroblasts [22, 24] at five days in UUO mouse kidneys. In UUO kidneys, quantification of cells co expressing the epithelial marker E-cadherin and the mesenchymal-cell marker αSMA revealed significantly increased cells undergoing EMT when compared with the control kidneys (**Figure 3A**, **3B**). Compared to sevoflurane+UUO kidneys, propofol+UUO kidneys had significantly fewer cells undergoing EMT (**Figure 3A**, **3B**).

Western blotting revealed suppressed E-cadherin protein levels in UUO mouse kidneys and increased levels of the mesenchymalcell markers αSMA and SM22α, indicating that UUO kidneys under went significant EMT when compared with control kidneys (**Figure 3C-F**). Compared to sevoflurane, propofol increased E-cadherin levels and decreased αSMA and SM22α levels in UUO kidneys, indicating that propofol inhibits EMT in early UUO mouse kidney (**Figure 3C-F**). The qPCR results were similar (**Figure 3G**, **3H**).

Propofol inhibited EMT and iNOS in HK-2 cells

In HK-2 cells, propofol pre-treatment suppressed TGF-β1-induced p-Smad3 (**Figure 4A**, **4B**). TGF-β1 suppressed E-cadherin with concomitant SM22α upregulation, suggesting that TGF-β1 induces EMT (**Figure 4C-E**); propofol pre-treatment inhibited TGF-β1-induced EMT (**Figure 4C-E**). As TGF-β1 is required for NF-κB-mediated modulation of iNOS activity when controlling the induction of the Epstein-Barr virus replication cycle [25], we also examined the expression of iNOS, a major enzyme for NO biosynthesis after stress. The TGF-β1 induced-iNOS protein levels were suppressed by propofol pre-treatment (**Figure 4F**). Furthermore, qPCR also revealed that propofol pre-treatment alleviated the TGF-β1 suppressed E-cadherin mRNA levels and suppressed the TGF-β1-induced SM22α mRNA levels (**Figure 4G**, **4H**).

Propofol ameliorated kidney fibrosis and suppressed EMT by regulating miR-155 in vivo and in vitro

MiR-155 expression increases during TGF-β-induced EMT in mammary epithelial cells through Smad4-mediated transcriptional upregulation, facilitating the loss of cell polarity and tight junctions [8]. Furthermore, miR-155 regulates iNOS induction [26]. To find the propofol mechanism of renal protection in UUO, we analyzed miR-155 levels*in vitro* and*in vivo*. Sham+sevoflurane mouse kidneys had higher miR-155 levels than sham+propofol mouse kidneys, but were not significantly different. Compared to the controls, UUO mouse kidneys had higher miR-155 levels at day 5, while miR-155 was significantly suppressed in kidney of propofol treated UUO mouseas compared to sevoflurane treated UUO mouse (**Figure 5A**). However, the effects of propofol and sevoflurane on miR-155 levels in UUO mouse kidney sat 28 days were not significantly different (Supplementary Figure 2C).

In HK-2 cells, propofol suppressed TGF-β1-induced miR-155 (**Figure 5B**). To analyze the role of miR-155 in EMT, we treated HK-2 cells with mimic-miR155 or antagomir-miR155. When compared to control group, mimic-miR155 treated HK-2 cells exhibited an increased E-cadherin protein expression and a decreased SM22α protein expression, which indicated an induction of EMT, such induced-EMT was inhibited by propofol treatment (**Figure 5C-E**); also the mimic-miR155 induced iNOS protein levels were inhibited by propofol treatment (**Figure 5C-F**). On the contrary, antagomir-miR155 suppressed TGF-β1-induced EMT and iNOS in HK-2 cells (**Figure 5G-J**). Taken together, these results reveal that miR-155 plays an important role in EMT and in iNOS protein induction, and that propofol inhibition of EMT occurs through miR-155 level regulation.

Discussion

Inhibition of kidney fibrosis is a fundamental process in research ondeveloping therapies against kidney disease. Although kidney fibroblasts have been implicated in kidney fibrosis-pathogenesis, inoculating only kidney fibroblasts as therapeutic targets would be challenging. In our analysis, propofol exhibits a renoprotection in UUO mice, which inhibits EMT and iNOS by regulating miR-155 levels.

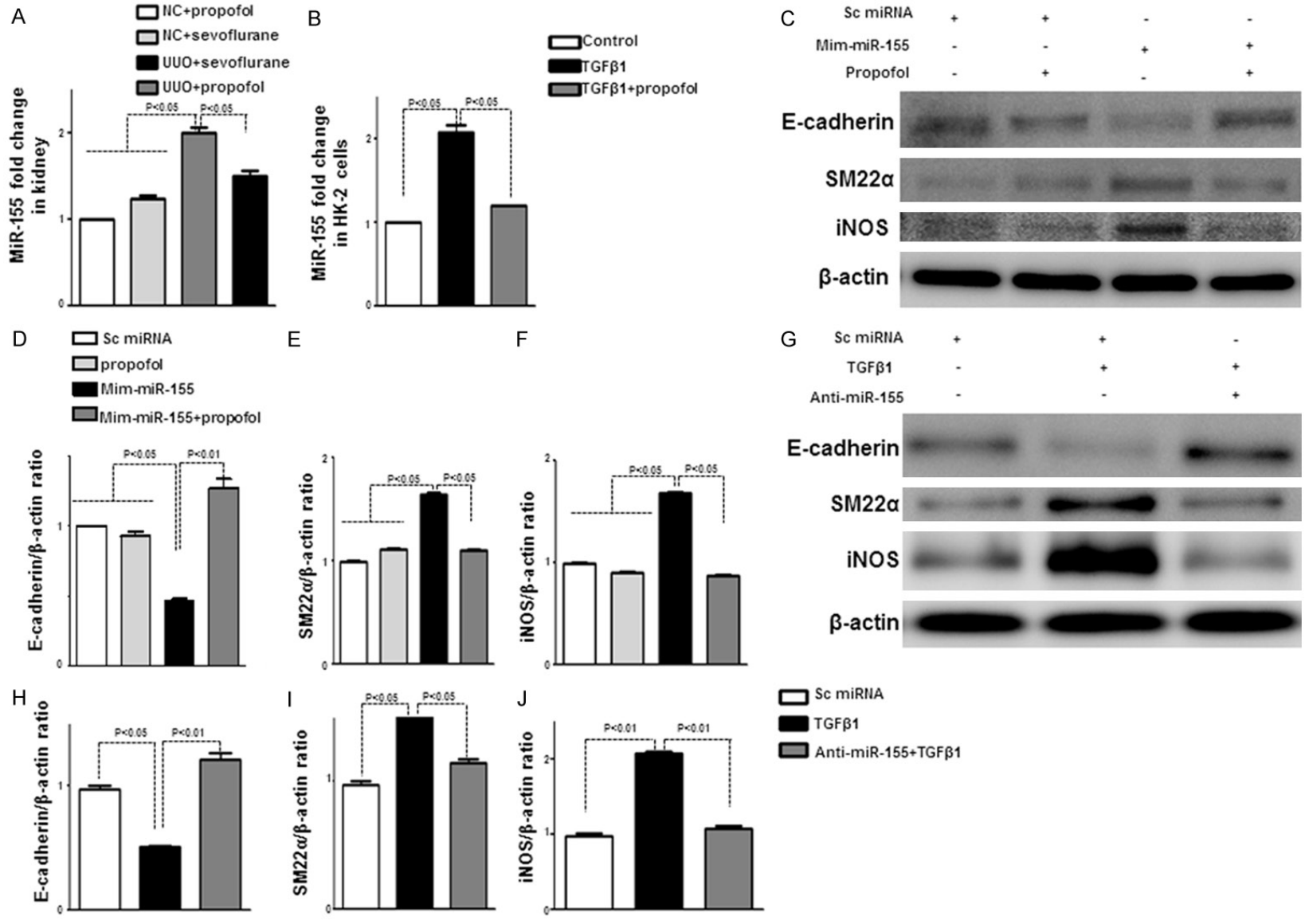

Figure 5. Propofol ameliorates kidney fibrosis and suppresses EMT by regulating miR-155 *in vivo* and *in vitro*. A. Kidney miR-155 levels were measured using semi-quantitative real-time RT-PCR (n = 5 per group). B. MiR-155 levels were analyzed in control HK-2 cells and HK-2 cells treated with propofol with or without TGF-β1. C. Western blot analysis of cell lysis. HK-2 cells were transfected with mimic-miR155 with or without propofol; E-cadherin, SM-22, and iNOS levels were analyzed. D-F. Densitometric analysis of E-cadherin, SM-22α, and iNOS normalized to β-actin (n = 4 per group). Data are the means ± SEM. G. Western blot analysis of cell

lysis. HK-2 cells were transfected with antagomir-miR155 with or without TGF-β1; E-cadherin, SM-22α, and iNOS levels were analyzed. H-J. Densitometric analysis of E-cadherin, SM-22α, and iNOS normalized to β-actin (*n* = 4 per group). Data are the means ± SEM.

UUO induces functional and pathological changes in the obstructed kidney, characterized by developing hydronephrosis, renal atrophy, remarkable renal weight loss, interstitial fibrosis, and renal dysfunction [27]. Compared with the controlson day 5, the UUO mouse model exhibit asevere kidney fibrosis, with significantly enlarged glomeruli, mesangial expansion, and relative areas of MTS-positive interstitial fibrosis. TGF-β is upregulated in response to injurious stimuli such as UUO, causing renal fibrosis associated with renal tubule EMT and ECM synthesis [28]. We found significantly increased TGF-β1 protein/mRNA levelsand p-Smad3 levels in UUO mouse kidneys as compared with the controls. Furthermore, UUO mouse kidneys had increased EMT-positive cells, which accompanied with suppression of E-cadherin and induction of SM22α or αSMA when compared with control mice. These data confirmed that EMT and TGF-β/Smad signaling playan important role in kidney fibrosis.

Chemically similar to a phenol-based free radical scavenger, propofol protects against oxidative stress in renal ischemia-reperfusion injury; propofol significantly reduces tissue necrosis [29]. Another report has suggested that, in humans, propofolhas antioxidant effects following kidney transplantation, and the authors examined the impact of renal transplantation on oxidative stress and inflammation by measuring changes in 8-iso-prostaglandin F2α (PGF2α) and 15-ketodihydro-PGF2α levels, respectively [30]. We found that propofol ameliorated kidney fibrosis, accompanied by decreased serum creatinine and BUN levels; this protection is associated with suppressed TGF-β/Smad3 signaling and NO levels; furthermore, propofol suppresses EMT. Our *in vitro* data also confirm that propofol suppresses TGF-β1-induced EMT and iNOS expression. EMT plays essential roles in renal fibrosis pathogenesis; it is commonly considered the major mechanism leading to renal fibrosis in CKD injury. We are first to report that propofol suppresses EMT in fibrotic mouse kidney and HK-2 cells. It also confirms the safety of propofol on the renal system during surgery.

Our most important finding is that propofol suppresses miR-155 *in vivo* and *in vitro*. The role of miR-155 in regulating the inflammatory response have be well documented in some models such as experimental autoimmune encephalomyelitis [31], graft-versus-host disease [32], alcoholic liver disease [33], and rheumatoid arthritis [34]. Acute renal injury (AKI) also results in significantly upregulated miR-155 in kidney tissue [35], and miR-155 may play an important role in TGF-β1-induced EMT and cell migration and invasion by targeting RhoA [8]. Our findings further confirm the important role of miR-155 in TGF-β1-induced EMT and iNOS induction. Although the iNOS gene has not been predicted as adirect miR-155 target gene, miR-155 might target its upstream regulator to indirectly suppress its expression [36]. In UUO, miR-155 regulation is the possible mechanism of propofol amelioration of kidney fibrosis.

Interestingly, the suppressed kidney fibrosis and EMT was only observed in early UUO; at 28 days, propofol did not prevent kidney fibrosis or EMT. There are several possible reasons for this: 1) the UUO model is a progressive kidney fibrosis model with increased TGF-β1 levels; inlate UUO, propofol cannot suppress TGF-β1 levels, consequently itcannot ameliorate EMT and kidney fibrosis; 2) NO production modifies renal hemodynamics in early-phase UUO and functions as an antifibrotic factor in chronic-phase UUO, which is likely due to the progressive downregulation of endogenous renal iNOS activity because of UUO; both pro-apoptotic and anti-apoptotic effects of NO have been demonstrated so far. Ina transgene mouse-model, the obstructed kidney exhibited higher iNOS activity until day 7 post-UUO as compared with day 0. However, the obstructed kidneys of wild-type mice exhibited significantly lower iNOS activity and protein at day 14 compared with day 0 [13]. We also found that NO and iNOS levels were higher in UUO mouse kidney at day 5; at day 28, the levels were decreased as compared to the controls (Supplementary Figure 2A, 2B).

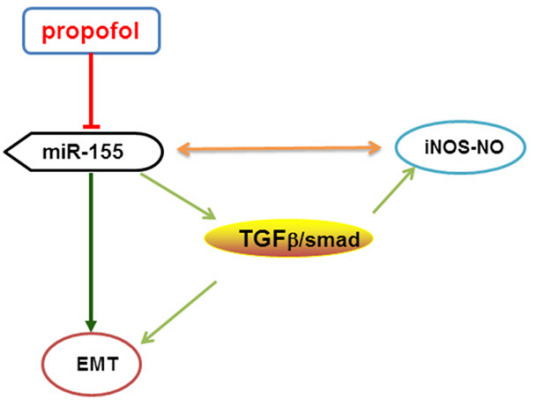

Figure 6. Possible mechanism of propofol on kidney fibrosis in early UUO mice. In early UUO mice, propofol may inhibit TGF-β1 expression and iNOS-NO production, consequently inhibiting EMT and kidney fibrosis byregulating miR-155.

Although our findings suggest that propofol is a promising anesthetic agent in fighting the UUO-induced kidney fibrosis, our study had limitations. We did not have a negative control group because it is not possible to perform this type of surgical intervention in mice without anesthesia.

To conclude, propofol attenuates renal fibrosis *in vivo*, which has potential clinical implications. In early UUO in mice, propofol may inhibit TGF-β1 expression and iNOS-NO production, consequently inhibiting EMT and kidney fibrosis by regulating miR-155 levels (**Figure 6**). However, further *in vivo* and *in vitro* studies are needed to elucidate the protective mechanism involved and to establish the optimally protective concentration range of propofol in humans.

Acknowledgements

Li Song performed the research and wrote the paper. Sen Shi contributed important reagents and assisted in writing the paper. Wei Jiang and Xueru Liu contributed to the animal experiments and collected and analyzed data. Yanzheng He designed the research.

Disclosure of conflict of interest

None.

Address correspondence to: Yanzheng He, Department of Vascular and Thyroid Surgery, Affiliated Hospital of Southwest Medical University, Luzhou 646000, Sichuan, China. Tel: +86 18989135750; Fax: +86 830-2392753; E-mail: lyhyz1965@163.com

References

[1] Kanasaki K, Taduri G and Koya D. Diabetic nephropathy: the role of inflammation in fibroblast activation and kidney fibrosis. Front Endocrinol (Lausanne) 2013; 4: 7.

[2] Eddy AA and Neilson EG. Chronic kidney disease progression. J Am Soc Nephrol 2006; 17: 2964-2966.

[3] Meng XM, Chung AC and Lan HY. Role of the TGF-beta/BMP-7/Smad pathways in renal diseases. Clin Sci (Lond) 2013; 124: 243-254.

[4] Thiery JP, Acloque H, Huang RY and Nieto MA. Epithelial-mesenchymal transitions in development and disease. Cell 2009; 139: 871-890.

[5] Kalluri R and Weinberg RA. The basics of epithelial-mesenchymal transition. J Clin Invest 2009; 119: 1420-1428.

[6] Jiang YS, Jiang T, Huang B, Chen PS and Ouyang J. Epithelial-mesenchymal transition of renal tubules: divergent processes of repairing in acute or chronic injury? Med Hypotheses 2013; 81: 73-75.

[7] Bartel DP. MicroRNAs: genomics, biogenesis, mechanism, and function. Cell 2004; 116: 281-297.

[8] Kong W, Yang H, He L, Zhao JJ, Coppola D, Dalton WS and Cheng JQ. MicroRNA-155 is regulated by the transforming growth factor beta/Smad pathway and contributes to epithelial cell plasticity by targeting RhoA. Mol Cell Biol 2008; 28: 6773-6784.

[9] Huang Y, Liu Y, Li L, Su B, Yang L, Fan W, Yin Q, Chen L, Cui T, Zhang J, Lu Y, Cheng J, Fu P and Liu F. Involvement of inflammation-related miR-155 and miR-146a in diabetic nephropathy: implications for glomerular endothelial injury. BMC Nephrol 2014; 15: 142.

[10] Runzer TD, Ansley DM, Godin DV and Chambers GK. Tissue antioxidant capacity during anesthesia: propofol enhances in vivo red cell and tissue antioxidant capacity in a rat model. Anesth Analg 2002; 94: 89-93, table of contents.

[11] Dikmen B, Yagmurdur H, Akgul T, Astarci M, Ustun H and Germiyanoglu C. Preventive effects of propofol and ketamine on renal injury in unilateral ureteral obstruction. J Anesth 2010; 24: 73-80.

[12] Zhai YP, Lu Q, Liu YW, Cheng Q, Wei YQ, Zhang F, Li CL and Yin XX. Over-production of nitric oxide by oxidative stress-induced activation of the TGF-beta1/PI3K/Akt pathway in mesangial cells cultured in high glucose. Acta Pharmacol Sin 2013; 34: 507-514.

[13] Miyajima A, Chen J, Poppas DP, Vaughan ED Jr. and Felsen D. Role of nitric oxide in renal tubu-

lar apoptosis of unilateral ureteral obstruction. Kidney Int 2001; 59: 1290-1303.
[14] Alves HC, Valentim AM, Olsson IA and Antunes LM. Intraperitoneal propofol and propofol fentanyl, sufentanil and remifentanil combinations for mouse anaesthesia. Lab Anim 2007; 41: 329-336.
[15] Shi S, Srivastava SP, Kanasaki M, He J, Kitada M, Nagai T, Nitta K, Takagi S, Kanasaki K and Koya D. Interactions of DPP-4 and integrin beta1 influences endothelial-to-mesenchymal transition. Kidney Int 2015; 88: 479-489.
[16] Lee YM, Shin JW, Lee EH, Moon Y, Seo YJ, Kim JY and Kim JU. Protective effects of propofol against hydrogen peroxide-induced oxidative stress in human kidney proximal tubular cells. Korean J Anesthesiol 2012; 63: 441-446.
[17] Green LC, Wagner DA, Glogowski J, Skipper PL, Wishnok JS and Tannenbaum SR. Analysis of nitrate, nitrite, and [15N]nitrate in biological fluids. Anal Biochem 1982; 126: 131-138.
[18] Meng XM, Tang PM, Li J and Lan HY. TGF-beta/Smad signaling in renal fibrosis. Front Physiol 2015; 6: 82.
[19] Levine DZ. Hyperfiltration, nitric oxide, and diabetic nephropathy. Curr Hypertens Rep 2006; 8: 153-157.
[20] Anjaneyulu M and Chopra K. Effect of irbesartan on the antioxidant defence system and nitric oxide release in diabetic rat kidney. Am J Nephrol 2004; 24: 488-496.
[21] Sefi M, Fetoui H, Soudani N, Chtourou Y, Makni M and Zeghal N. Artemisia campestris leaf extract alleviates early diabetic nephropathy in rats by inhibiting protein oxidation and nitric oxide end products. Pathol Res Pract 2012; 208: 157-162.
[22] LeBleu VS, Taduri G, O'Connell J, Teng Y, Cooke VG, Woda C, Sugimoto H and Kalluri R. Origin and function of myofibroblasts in kidney fibrosis. Nat Med 2013; 19: 1047-1053.
[23] Meran S and Steadman R. Fibroblasts and myofibroblasts in renal fibrosis. Int J Exp Pathol 2011; 92: 158-167.
[24] Kalluri R and Neilson EG. Epithelial-mesenchymal transition and its implications for fibrosis. J Clin Invest 2003; 112: 1776-1784.
[25] Oussaief L, Ramirez V, Hippocrate A, Arbach H, Cochet C, Proust A, Raphael M, Khelifa R and Joab I. NF-kappaB-mediated modulation of inducible nitric oxide synthase activity controls induction of the Epstein-Barr virus productive cycle by transforming growth factor beta 1. J Virol 2011; 85: 6502-6512.
[26] Wang X, Zhao Q, Matta R, Meng X, Liu X, Liu CG, Nelin LD and Liu Y. Inducible nitric-oxide synthase expression is regulated by mitogen-activated protein kinase phosphatase-1. J Biol Chem 2009; 284: 27123-27134.
[27] Klahr S and Morrissey J. Obstructive nephropathy and renal fibrosis. Am J Physiol Renal Physiol 2002; 283: F861-875.
[28] Qu X, Jiang M, Sun YB, Jiang X, Fu P, Ren Y, Wang D, Dai L, Caruana G, Bertram JF, Nikolic-Paterson DJ and Li J. The Smad3/Smad4/CDK9 complex promotes renal fibrosis in mice with unilateral ureteral obstruction. Kidney Int 2015; 88: 1323-1335.
[29] Wang HH, Zhou HY, Chen CC, Zhang XL and Cheng G. Propofol attenuation of renal ischemia/reperfusion injury involves heme oxygenase-1. Acta Pharmacol Sin 2007; 28: 1175-1180.
[30] Basu S, Meisert I, Eggensperger E, Krieger E and Krenn CG. Time course and attenuation of ischaemia-reperfusion induced oxidative injury by propofol in human renal transplantation. Redox Rep 2007; 12: 195-202.
[31] Murugaiyan G, Beynon V, Mittal A, Joller N and Weiner HL. Silencing microRNA-155 ameliorates experimental autoimmune encephalomyelitis. J Immunol 2011; 187: 2213-2221.
[32] Ranganathan P, Heaphy CE, Costinean S, Stauffer N, Na C, Hamadani M, Santhanam R, Mao C, Taylor PA, Sandhu S, He G, Shana'ah A, Nuovo GJ, Lagana A, Cascione L, Obad S, Broom O, Kauppinen S, Byrd JC, Caligiuri M, Perrotti D, Hadley GA, Marcucci G, Devine SM, Blazar BR, Croce CM and Garzon R. Regulation of acute graft-versus-host disease by microRNA-155. Blood 2012; 119: 4786-4797.
[33] Bala S, Marcos M, Kodys K, Csak T, Catalano D, Mandrekar P and Szabo G. Up-regulation of microRNA-155 in macrophages contributes to increased tumor necrosis factor {alpha} (TNF{alpha}) production via increased mRNA half-life in alcoholic liver disease. J Biol Chem 2011; 286: 1436-1444.
[34] Leng RX, Pan HF, Qin WZ, Chen GM and Ye DQ. Role of microRNA-155 in autoimmunity. Cytokine Growth Factor Rev 2011; 22: 141-147.
[35] Saikumar J, Hoffmann D, Kim TM, Gonzalez VR, Zhang Q, Goering PL, Brown RP, Bijol V, Park PJ, Waikar SS and Vaidya VS. Expression, circulation, and excretion profile of microRNA-21, -155, and -18a following acute kidney injury. Toxicol Sci 2012; 129: 256-267.
[36] Cardoso AL, Guedes JR, Pereira de Almeida L and Pedroso de Lima MC. miR-155 modulates microglia-mediated immune response by down-regulating SOCS-1 and promoting cytokine and nitric oxide production. Immunology 2012; 135: 73-88.

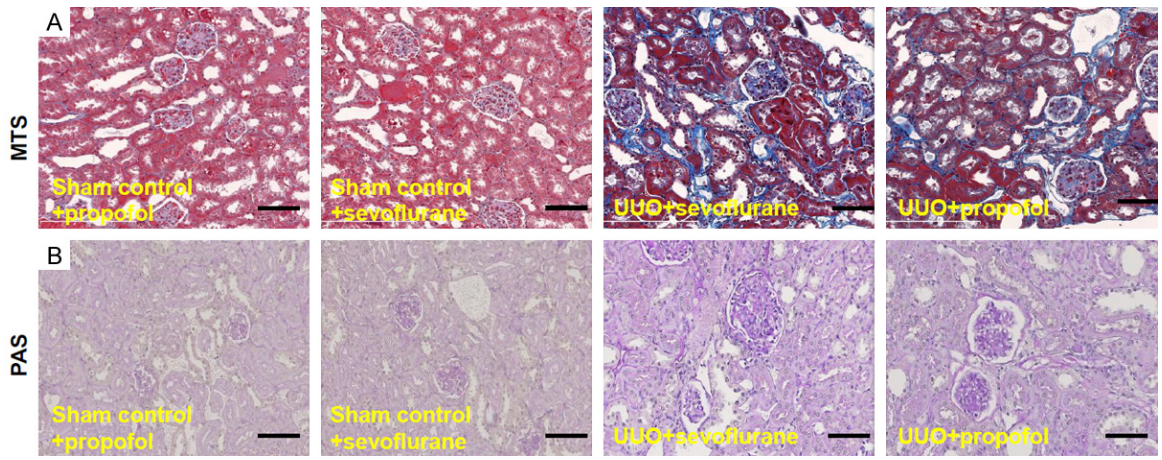

Supplementary Figure 1. Propofol can not amelioration of kidney fibrosis in later periods of UUO mice (day 28). A: MTS staining for kidney of of the indicated group of mice. B: PAS staining in kidney of the indicated group of mice. Scale bar: 50 μm. N = 5 were analyzed.

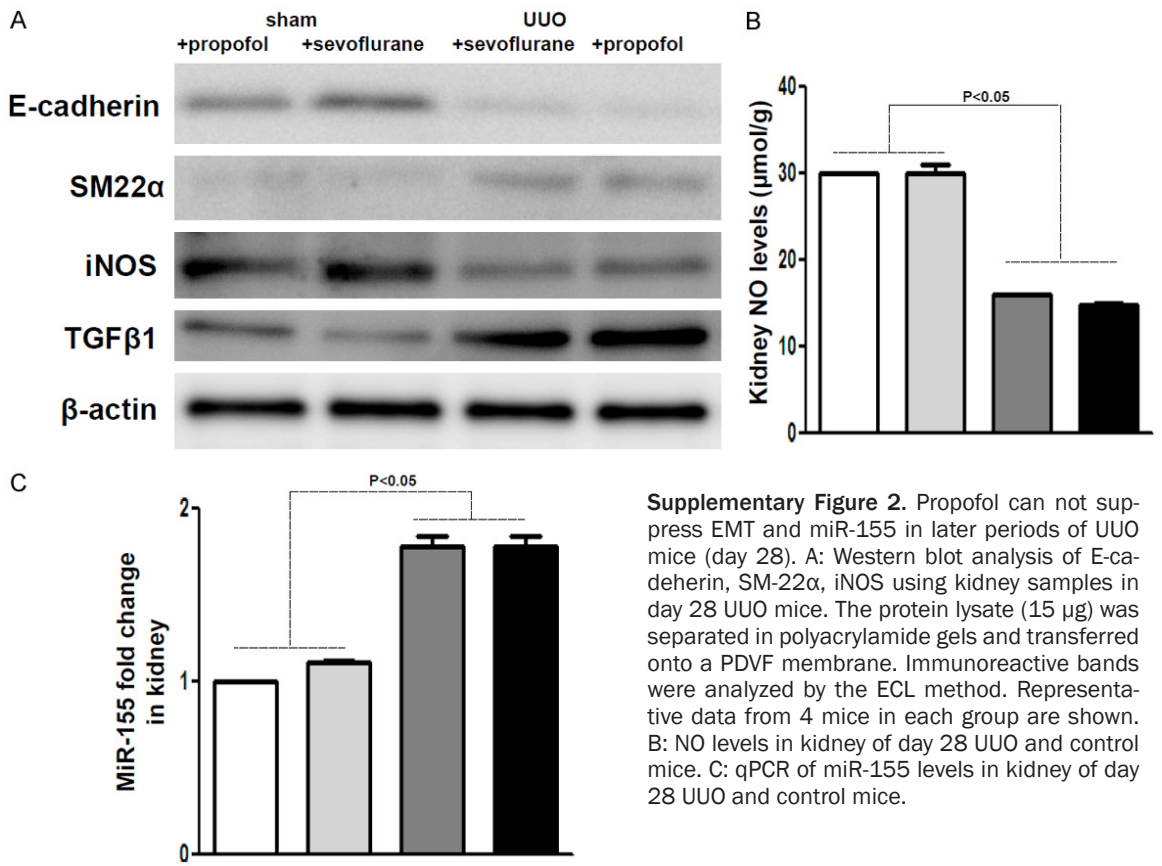

Supplementary Figure 2. Propofol can not suppress EMT and miR-155 in later periods of UUO mice (day 28). A: Western blot analysis of E-cadeherin, SM-22α, iNOS using kidney samples in day 28 UUO mice. The protein lysate (15 μg) was separated in polyacrylamide gels and transferred onto a PDVF membrane. Immunoreactive bands were analyzed by the ECL method. Representative data from 4 mice in each group are shown. B: NO levels in kidney of day 28 UUO and control mice. C: qPCR of miR-155 levels in kidney of day 28 UUO and control mice.